

Polarization recovery in lead zirconate titanate thin films deposited on nanosheets-buffered Si (001)

Anuj Chopra,¹ Muharrem Bayraktar,^{2,3} Maarten Nijland,¹
Johan E. ten Elshof,¹ Fred Bijkerk,³ and Guus Rijnders^{1,a}

¹*Inorganic Materials Science Group, MESA+ Institute for Nanotechnology,
University of Twente, PO Box 217, 7500 AE Enschede, The Netherlands*

²*Laser Physics and Nonlinear Optics Group, MESA+ Institute for Nanotechnology,
University of Twente, PO Box 217, 7500 AE Enschede, The Netherlands*

³*Industrial Focus Group XUV Optics, MESA+ Institute for Nanotechnology,
University of Twente, PO Box 217, 7500 AE Enschede, The Netherlands*

(Received 5 October 2016; accepted 20 November 2016; published online 16 December 2016)

Fatigue behavior of $\text{Pb}(\text{Zr,Ti})\text{O}_3$ (PZT) films is one of the deterrent factors that limits the use of these films in technological applications. Thus, understanding and minimization of the fatigue behavior is highly beneficial for fabricating reliable devices using PZT films. We have investigated the fatigue behavior of preferentially oriented PZT films deposited on nanosheets-buffered Si substrates using LaNiO_3 bottom and top electrodes. The films show fatigue of up to 10% at 100 kHz, whereas no fatigue has been observed at 1 MHz. This frequency dependence of the fatigue behavior is found to be in accordance with Dawber–Scott fatigue model that explains the origin of the fatigue as migration of oxygen vacancies. Interestingly, a partial recovery of remnant polarization up to ~97% of the maximum value is observed after 4×10^9 cycles which can be further extended to full recovery by increasing the applied electric field. This full recovery is qualitatively explained using kinetic approach as a manifestation of depinning of domains walls. The understanding of the fatigue behavior and polarization recovery that is explained in this paper can be highly useful in developing more reliable PZT devices. © 2016 Author(s). All article content, except where otherwise noted, is licensed under a Creative Commons Attribution (CC BY) license (<http://creativecommons.org/licenses/by/4.0/>). [<http://dx.doi.org/10.1063/1.4971373>]

INTRODUCTION

Lead zirconate titanate (PZT) is an extensively investigated material because of its potential use in ferroelectric non-volatile memory devices, pyroelectric detectors and piezoelectrically-driven microelectromechanical systems.^{1–5} Stability of the ferroelectric and piezoelectric properties such as switchable polarization is a key requisite in long term operation of these devices. However, it is observed that the switchable polarization of PZT films decreases when the PZT films are used for increased number of bipolar-voltage cycles.^{6–10} This reduction in the switchable/remnant polarization, i.e. fatigue, limits the reliability and usage of the PZT films in device applications.

Despite having numerous studies and proposed models on fatigue mechanism,^{6–10} physical origin of fatigue is still debatable. In general, fatigue is explained as a manifestation of the accumulation of oxygen vacancies at the electrode/ferroelectric film interface during the switching cycles and pinning of the domain walls by these vacancies.^{11–15} Understanding the role of these two contributions to fatigue behavior is quite intriguing and highly desirable in order to improve the performance of PZT films. Fatigue has been reported mostly in PZT films with Pt electrodes where a sharp decay in switchable polarization occurs within 10^8 cycles of polarization switching. This decay is imputed to the pinning of the domain wall motion due to oxygen vacancies and/or charged point defects.^{16–20}

^aGuus Rijnders (a.j.h.m.rijnders@utwente.nl)

During repeated switching cycles, it is assumed that oxygen vacancies and other point defects in PZT thin films move and accumulate near the PZT-electrode interfaces. This accumulation results in screening of the polarization which induces a decay in the remnant polarization. It is reported that use of conductive metal oxides such as RuO_2 , IrO_2 and SrRuO_3 (SRO) could reduce the fatigue substantially by letting the oxygen vacancies diffuse into the electrodes.²¹⁻²⁵ This diffusion process results in reduced screening of polarization and thereby improved fatigue response. However, Pintilie *et. al.* have reported otherwise where fatigue occurred in epitaxial PZT films with SRO electrodes deposited on SrTiO_3 substrates.¹⁰ In the same paper, a partial recovery of the remnant polarization was reported with a conclusion that further detailed investigations will be required for a clear understanding of the topic. However, it is still an open and intriguing question to know the origins and extent of fatigue and polarization recovery.

In this work, a systematic study of the fatigue behavior has been conducted for PZT films with LaNiO_3 (LNO) electrodes deposited on nanosheets-buffered Si substrates. Fatigue is found to be highly frequency dependent and observed only at 100 kHz cycling, but not at 1 MHz cycling. This frequency dependent behavior is explained using Dawber–Scott fatigue model that relates the fatigue to the frequency dependent movement of oxygen vacancies.^{13,14} After the fatigued state, a partial recovery of the remnant polarization up to $\sim 97\%$ of the maximum value is observed, which is explained as a result of the diffusion of the oxygen vacancies to the electrodes. The partial recovery can be further enhanced to full recovery by application of a higher electric field. This full recovery of the remnant polarization is qualitatively explained using kinetic approach²⁶ as a manifestation of depinning of domains walls.

EXPERIMENTAL RESULTS

In preparing the samples, ubiquitously available Si (001) substrates are used. Direct integration of PZT films onto natively oxidized Si substrates is a challenging task due to the inter-diffusion and the large mismatch between the lattice parameters of the film and the substrate.^{27,28} In this work, PZT films were integrated on natively oxidized Si substrates using TiO_x (TO) nanosheets as a buffer layer. TO-nanosheets were deposited from their colloidal solution using Langmuir–Blodgett process. Details about the preparation of TO-nanosheets can be found elsewhere.²⁹ As the bottom and top electrodes, LNO was used due to its high conductivity. PZT with a [Zr/Ti] ratio of [52/48] was investigated in this study. LNO and PZT films (thicknesses of 200 nm and 750 nm, respectively) were fabricated by pulsed laser deposition that uses a KrF excimer laser (wavelength 248 nm, pulse duration 20 ns). The bottom LNO layer was deposited at a temperature of 600 °C in an oxygen pressure of 0.140 mbar. The subsequent PZT and LNO layers were deposited at 575 °C in 0.270 mbar and 0.140 mbar oxygen pressure, respectively. More details about pulsed laser fabrication process and subsequent structural characterization using XRD and SEM can be found elsewhere.^{30,31} A 100 nm thick Pt layer was sputtered on LNO top electrode by radio frequency sputtering at room temperature to increase the homogeneity of the electric field.

In order to facilitate the electrical measurements, the top electrode was patterned into capacitors of $200 \times 200 \mu\text{m}^2$ area using standard photolithography process and structured by argon ion-etching. The hysteresis and fatigue measurements were performed using the TF-2000 Analyzer (aixACCT Systems GmbH) as schematically shown in Fig. 1 (a). The electrical signals used to measure the dynamic hysteresis loops and fatigue behavior are shown schematically in Fig. 1(b). The dynamic hysteresis loops were measured with an electric field amplitude ranging from 389 kV/cm to 918 kV/cm at a frequency of 1 kHz. The fatigue investigations were performed by applying bipolar square pulses of 265 kV/cm and 332 kV/cm amplitude at 100 kHz and 1 MHz frequency, respectively. It is well known that samples fatigued at higher frequencies demand higher excitation amplitudes since sample relaxation, time constant and the driving power of set up limit the switching of polarization. Thus, at 1 MHz these effects were compensated by increasing the amplitude of fatigue signal to 332 kV/cm to make sure that the tested sample is fully switched.

Figure 2(a) shows a detailed plot of the dependence of remnant polarization (positive as well as negative) to the number of fatigue cycles at 100 kHz and 1 MHz.³² Although the polarization values for two frequencies are almost the same in the first cycle, their behavior is completely different

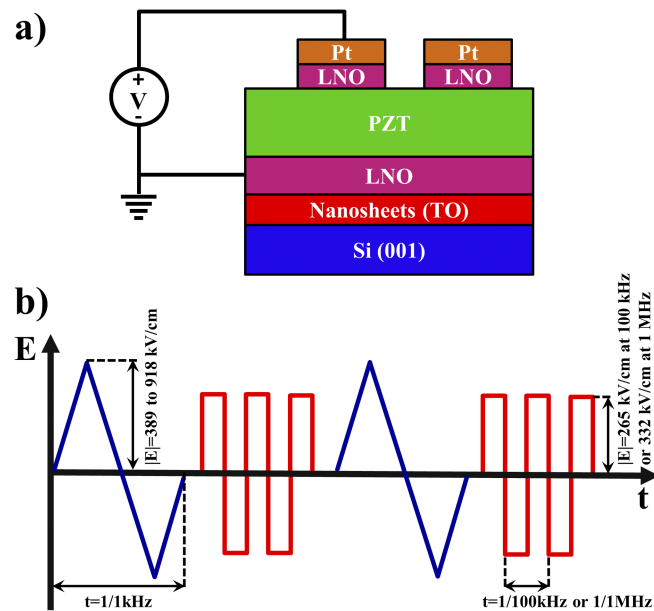


FIG. 1. (a) Schematic of ferroelectric capacitor structure and (b) the signals used for the fatigue and dynamic measurements.

with the increase in fatigue cycles. There is a small visible decay in the polarization for 1 MHz signal which reveals a rather stable operation with the increase in number of cycles. However, for the 100 kHz signal the remnant polarization increases and reaches to a maximum value of $(P_{r+} - P_{r-})/2 = 20.7 \mu\text{C}/\text{cm}^2$ at around 2×10^8 cycles. For a detailed investigation of this increase, switching current transients versus electric field (I - E loops) are measured for different number of fatigue cycles, $N = 0, 1 \times 10^5, 2 \times 10^8$, as shown in Fig. 2(b). The peak positions in the I - E curves correspond to the coercive field required for switching the domains in either direction. Appearance of double peaks both in forward and backward direction suggests the existence of two different kinds of domains with E_{cf}^1, E_{cf}^2 coercive electric fields in the forward direction and E_{cb}^1, E_{cb}^2 in the backward direction. However, current peaks of two domains merge and I - E curves with single switching peak in both directions are obtained after 2×10^8 fatigue cycles. The new switching peak is much sharper than the previous peaks and occurs at lower coercive field in both of the directions as compared to E_{cf}^1 and E_{cb}^1 . This polarization increase observed at 100 kHz in the early stage of the fatigue cycles has been reported both theoretically and experimentally in the literature.³³ It is explained as a manifestation of increased volume fraction of depinned domain walls under the application of a bipolar field which is evident by the sharp increase in the current peak between 1×10^5 - 2×10^8 fatigue cycles.

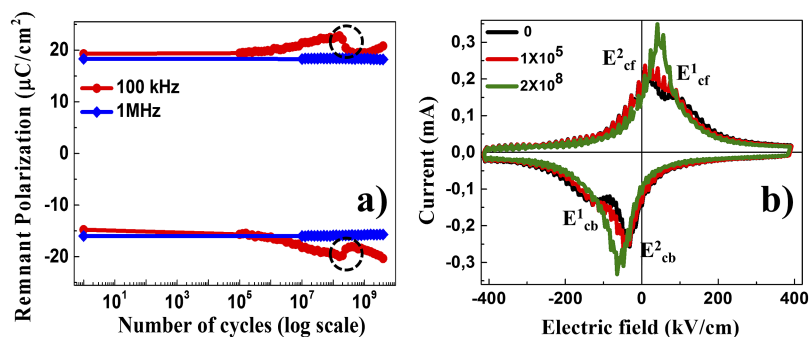


FIG. 2. (a) Fatigue measurements in PZT films at 100 kHz and 1 MHz frequencies. The black color circles are highlighting the decay in remnant polarization for the measurements conducted between 2×10^8 and 4×10^8 fatigue cycles. (b) Macroscopic switching current-electric field data measured for 100 kHz fatigued sample. The pristine loop reveals double switching peaks which later merge to a single peak after 2×10^8 fatigue cycles.

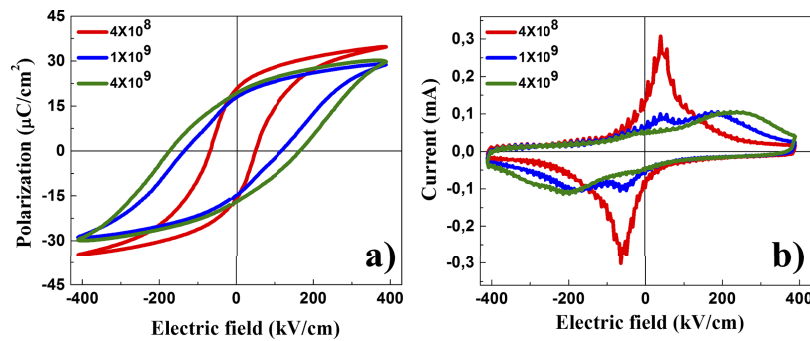


FIG. 3. (a) Macroscopic polarization-electric field hysteresis loops recorded for 4×10^8 , 1×10^9 and 4×10^9 fatigue cycles. (b) Switching current-electric field curves of the respective hysteresis loops.

The remnant polarization shows a decay of $\sim 10\%$ from the maximum value between 2×10^8 and 4×10^8 fatigue cycles as shown in the encircled region in Fig. 2(a). Interestingly, a partial recovery of remnant polarization up to $\sim 97\%$ of the maximum value is observed after 4×10^9 cycles. The polarization data (P - E loops) and switching current in the 4×10^8 - 4×10^9 range provides critical information regarding the fatigue kinetics as shown in Fig. 3. It is interesting to note that a significant increase in coercive field, from below 100 kV/cm up to around 200 kV/cm, is observed in the P - E hysteresis loops in Fig. 3(a) and the shape of the hysteresis loops become more slanted with increase in fatigue cycles. The increase in coercive field suggests formation of domains at higher coercive field, which can be better seen in the I - E loops shown in Fig. 3(b). It is clearly evident in Fig. 3(b) that the amplitude of the switching peak existing at lower coercive field (< 100 kV/cm) starts to decrease with increase in fatigue cycles. On the other hand, a new switching peak at much higher electric field (~ 200 kV/cm) emerges and its amplitude increases as the fatigue cycles are increased, confirming our observations from the P - E loops. This increasing trend in the current peak amplitude was confirmed not to be due to increase in leakage current. Low amplitude of the switching peaks depicts a partial switching of the capacitor at the present electric field. On applying a higher electric field, up to 918 kV/cm, it is observed that the switching peak observed at lower coercive field vanishes and the switching peak at higher coercive field is fully switched in both the directions as shown in Fig. 4(a). Interestingly, both remnant polarization and amplitude of the switching peak at high coercive field fully recovered to the previous maximum values as shown in Fig. 4(a-b) with application of higher electric field. Similar kind of polarization recovery by applying higher electric field has been reported previously for PZT films deposited on Pt electrodes, although no physical description for the occurrence is included.³⁴

The observed fatigue phenomenon and its recovery can be explained using Dawber-Scott model and kinetic approach of the fatigue. According to Dawber-Scott model the charged defects such as oxygen vacancies accumulate easily near film-electrode interfaces and results in the formation of

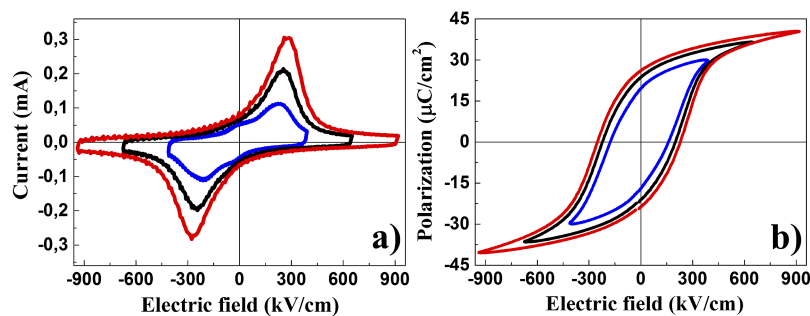


FIG. 4. (a) Switching current-electric field curves and (b) polarization-electric field hysteresis loops recorded at different electric fields recorded after 4×10^9 cycles.

space-charge layers under the influence of an external field. This makes the total film to behave as an n-p-n junction which results in screening of polarization, i.e. the remnant polarization reduces with increase in fatigue cycles. In addition, trapped charges in ferroelectrics are another potential source known for screening of the polarization. Under the combined effect of the oxygen vacancies and trapped charges, the polarization decays with increase in fatigue cycles. Another prediction of the Dawber-Scott model is that mobility/response of the oxygen vacancies and trapped charges is highly dependent on the frequency of the fatigue signal. Specifically, at higher frequencies neither the oxygen vacancies nor the deep traps respond to the applied electric field. Therefore, almost no change in remnant polarization is observed at 1 MHz frequency. However, at lower frequencies both the oxygen vacancies and trapped charges become active. Thus, at 100 kHz fatigue frequency, oxygen vacancies start to migrate toward top and bottom electrodes, resulting in the screening of polarization and subsequent decay in the remnant polarization. Once the migration process is complete, recovery process starts depending on the possibility of migration of oxygen vacancies and charge defects into the electrodes. The extent of recovery will depend on the amount of oxygen vacancy diffusion into the electrode. In the case of oxide electrodes such as LNO, the extent of diffusion is quite large as it is very evident from our fatigue measurements. However, there are still finite number of space charges (both oxygen vacancies and trapped charges) in the interface of PZT film and electrode which do not diffuse into the electrode and act as pinning centers. The pinning centers act as kinetically frozen regions in the PZT films due to insufficiency of the amplitude and period of the electric field for completing the switching event. Thus, polarization of the PZT films cannot recover completely as seen in the shape of the hysteresis loops observed at 4×10^9 cycles in Fig. 3(a). However, the pinning can be overcome by increasing the field amplitude as seen in Fig. 4. This result is in accordance to the kinetic model of fatigue.

In summary, a detailed study on fatigue behavior of PZT films sandwiched between LNO top and bottom electrodes have been performed. It is observed that fatigue properties were strongly frequency dependent which was explained using Dawber-Scott model. A partial recovery of the remnant polarization up to 97% of the maximum value is observed for the fatigue signal of 100 kHz. This partial recovery is explained as a manifestation of the diffusion of space charges into the LNO electrodes. During the recovery, splitting of switching current peaks is observed which is attributed to the pinning of the domains. The domain pinning was overcome by increasing the amplitude of the electric field, which is in accordance to the kinetic model of fatigue. Further detailed investigations to understand the influence of electrically active traps and oxygen vacancies in fatigue phenomena using different electrodes is underway.

ACKNOWLEDGMENTS

Authors A. Chopra and M. Bayraktar both contributed equally to this article. This research program is funded by “Stichting Technologie en Wetenschap (STW)” under the contract 10448 with the project name “Smart Multilayer Interactive Optics for Lithography at Extreme UV wavelengths (SMILE)”. The authors would like to thank Dr. Minh Nguyen for Pt coating.

¹ *Ferroelectric Thin Films*, edited by M. Okuyama and Y. Ishibashi (Springer-Verlag, Berlin Heidelberg, 2005).

² C. C. Chang and C. S. Tang, *Sens. Actuator B-Chem.* **65**, 171 (1998).

³ S. Trolier-McKinstry and P. Muralt, *Journal of Electroceramics* **12**, 7 (2004).

⁴ M. Bayraktar, W. A. Wessels, C. J. Lee, F. A. van Goor, G. Koster, G. Rijnders, and F. Bijkerk, *J. Phys. D: Appl. Phys.* **45**, 494001 (2012).

⁵ M. Bayraktar, A. Chopra, G. Rijnders, K. Boller, and F. Bijkerk, *Opt. Exp.* **22**, 30623 (2014).

⁶ H. M. Duiker, B. P. Beale, J. F. Scott, C. A. Paz de Araujo, B. M. Melnick, J. D. Cuchiaro, and L. D. McMillan, *J. Appl. Phys.* **68**, 5783 (1990).

⁷ M. Tajiri and H. Nozawa, *Jpn. J. Appl. Phys., Part 1* **40**, 5590 (2001).

⁸ A. K. Tagantsev, I. Stolichnov, E. L. Colla, and N. Setter, *J. Appl. Phys.* **90**, 1387 (2001).

⁹ K. T. Li and V. C. Lo, *J. Appl. Phys.* **97**, 034107 (2005).

¹⁰ L. Pintilie, I. Vrejoiu, D. Hesse, and M. Alexe, *Appl. Phys. Lett.* **88**, 102908 (2006).

¹¹ G. Arlt and U. Robels, *Integr. Ferroelectr.* **3**, 343 (1993).

¹² C. Brennan, *Ferroelectrics* **150**, 199 (1993).

¹³ M. Dawber and J. F. Scott, *Appl. Phys. Lett.* **76**, 1060 (2000).

¹⁴ M. Dawber and J. F. Scott, *Appl. Phys. Lett.* **76**, 3655 (2000).

¹⁵ B. G. Chae, C. H. Park, Y. S. Yang, and M. S. Jang, *Appl. Phys. Lett.* **75**, 2135 (1999).

¹⁶ Y. Masuda and T. Nozaka, *Jpn. J. Appl. Phys., Part 1* **42**, 5941 (2003).

- ¹⁷ G. Asano, H. Morioka, and H. Funakubo, *Appl. Phys. Lett.* **83**, 5506 (2003).
- ¹⁸ S. Aggarwal, I. G. Jenkins, B. Nagaraj, C. J. Kerr, C. Canedy, R. Ramesh, G. Velasquez, L. Boyer, and J. T. Evans, Jr., *Appl. Phys. Lett.* **75**, 1787 (1999).
- ¹⁹ O. Auciello, K. D. Gifford, D. J. Lichtenwalner, R. Dat, H. N. Al-Shareef, K. R. Bellur, and A. Kingon, *Integrated Ferroelectrics* **6**, 173 (1995).
- ²⁰ M. Grossmann, D. Bolten, O. Lohse, U. Boettger, R. Waser, and S. Tiedke, *Appl. Phys. Lett.* **77**, 1894 (2000).
- ²¹ S. B. Majumder, Y. N. Mohapatra, and D. C. Agrawal, *Appl. Phys. Lett.* **70**, 138 (1997).
- ²² G. Le Rhun, G. Poullain, and R. Bouregba, *J. Appl. Phys.* **96**, 3876 (2004).
- ²³ I. Stolichnov, A. Tagantsev, N. Setter, J. S. Cross, and M. Tsukuda, *Appl. Phys. Lett.* **74**, 3552 (1999).
- ²⁴ W. Wu, K. H. Wong, C. L. Choy, and Y. H. Zhang, *Appl. Phys. Lett.* **77**, 3441 (2000).
- ²⁵ M. Kobune, O. Matsuura, T. Matsuzaki, A. Mineshige, S. Fujii, H. Fujisawa, M. Shimizu, and H. Niu, *Jpn. J. Appl. Phys., Part 1* **39**, 5451 (2000).
- ²⁶ V. Ya. Shur, E. L. Rumyantsev, E. V. Nikolaeva, E. I. Shishkin, and I. S. Baturin, *J. Appl. Phys.* **90**, 6312 (2001).
- ²⁷ A. Chopra, D. Pantel, Y. Kim, M. Alexe, and D. Hesse, *J. Appl. Phys.* **114**, 084107 (2013).
- ²⁸ A. Chopra, M. Alexe, and D. Hesse, *J. Appl. Phys.* **117**, 044102 (2015).
- ²⁹ M. Nijland, S. Kumar, R. Lubbers, D. H. A. Blank, G. Rijnders, G. Koster, and J. E. ten Elshof, *ACS Appl. Mater. Interfaces* **6**, 2777 (2014).
- ³⁰ A. Chopra, M. Bayraktar, F. Bijkerk, and G. Rijnders, *Thin Solid Films* **589**, 13 (2015).
- ³¹ M. Bayraktar, A. Chopra, F. Bijkerk, and G. Rijnders, *Appl. Phys. Lett.* **105**, 132904 (2014).
- ³² W. W. Iii, B. K. Gilbert, H. D. Chen, K. R. Udayakumar, L. E. Cross, and C. M. Bozler, *Integrated Ferroelectrics* **10**, 335 (1995).
- ³³ V. Ya. Shur, E. L. Rumyantsev, E. V. Nikolaeva, E. I. Shishkin, and I. S. Baturin, *Phys. Solid State* **44**, 2145 (2002).
- ³⁴ L. F. Schloss and P. C. McIntyre, *J. Appl. Phys.* **93**, 1743 (2003).